# The concentration, source and deposition flux of ammonium and nitrate in atmospheric particles during dust events at a coastal site in northern China

Jianhua Qi[1], Xiaohuan Liu[1], Xiaohong Yao[1], Ruifeng Zhang[1], Xiaojing Chen[1], Xuehui Lin[2], Huiwang Gao[1], Ruhai Liu[1]

[1]Key Laboratory of Marine Environment and Ecology, Ministry of Education, Ocean University of China, Qingdao, 266100, China

[2]Qingdao Institute of Marine Geology, Qingdao, 266100, China

Correspondence to: Jianhua Qi (qjianhua@ouc.edu.cn)

**Abstract.** Asian dust has been reported to carry anthropogenic reactive nitrogen during transport from source areas to the oceans. In this study, we attempted to characterize $NH_4^+$ and $NO_3^-$ in atmospheric particles collected at a coastal site in northern China during spring dust events from 2008 to 2011. Based on the mass concentrations of $NH_4^+$ and $NO_3^-$ in each total suspended particle (TSP) sample, the samples can be classified into increasing or decreasing types. In Category 1, the concentrations of $NH_4^+$ and $NO_3^-$ were 20%-440% higher in dust day samples relative to samples collected immediately before or after a dust event. These concentrations decreased by 10-75% in the dust day samples in Categories 2 and 3. Back trajectory analysis suggested that multiple factors such as the transport distance prior to the reception site, the mixing layer depth on the transport route and the residence time across highly polluted regions, might affect the concentrations of $NH_4^+$ and $NO_3^-$. $NH_4^+$ in the dust day samples was likely either in the form of ammonium salts existing separately with dust aerosols or as the residual of incomplete reactions between ammonium salts and carbonate salts. $NO_3^-$ in the dust day samples was attributed to various formation processes during the long-range transport. The positive matrix factorization (PMF) receptor model results showed that the contribution of soil dust increased from 23% to 36% on dust days with decreasing contributions from local anthropogenic inputs and associated secondary aerosols. The estimated deposition flux of $N_{NH4+-NO3-}$ varied greatly from event to event, e.g., the dry deposition flux of $N_{NH4+-NO3-}$ increased by 9-285% in Category 1, but decreased by 46%-73% in Category 2. In Categories 3, the average dry deposition fluxes of particulate nitrate and ammonium decreased by 46% and increased by 10%, respectively, leading

to 11-48% decrease in the fluxes of $N_{NH4++NO3-}$.

Keywords: aerosols, nitrogen, dust, source apportionment, dry deposition flux

## 1 Introduction

Reactive nitrogen carried in dust particles can be transported over a long distance, and the atmospheric nitrogen deposition in oceans has been recognized as an important external source of the nitrogen supporting phytoplankton growth (Duce et al., 2008; Zhang et al., 2010b). This hypothesis has been evaluated through incubation experiments, in situ experiments, and the use of satellite observational data (Banerjee and Kumar 2014; Guo et al., 2012; Liu et al., 2013; Shi et al., 2012; Tan and Wang, 2014). However, the process is dynamic due to the worldwide changing emissions of $NO_x$ and $NH_3$ in the last few decades. For example, China and most of the developing countries in Asia experienced a large increase in emissions of $NH_3$ and $NO_x$ while a substantial decrease in emissions occurred in Europe over the last three decades (Grice et al., 2009; Liu et al., 2017; Ohara et al., 2007; Skjøth and Hertel, 2013). The change would affect the nitrogen carried by dust particles to some extent, and updated studies are thereby essential.

Asian dust is one of three largest dust sources on earth. Asian dust has been reported to not only frequently cross over the mainland and the China Seas, but also to occasionally reach the remote northern Pacific Ocean or North America (Creamean 2013; Tan and Wang, 2014; Van Curen and Cahill, 2002; Zhang and Gao, 2007). In an extreme case, Asian dust was found to be transported more than one full circuit around the globe in approximately 13 days (Uno et al 2009). During the long-range transport, dust particles may mix with anthropogenic air pollutants and consequently undergo complicated chemical reactions (Cui et al., 2009; Li et al., 2014; Ma et al., 2012; Wang et al., 2011; Wang et al., 2016b; Wang et al., 2017a; Xu et al., 2014; Yang et al., 2002). For example, a few studies have shown that the concentrations of atmospheric particulate $NO_3^-$ and $NH_4^+$ on dust storm days were 2-5 times larger than those prior to the events in Beijing (Liu et al., 2014; Liu and Bei, 2016). Fitzgerald et al. (2015) found that almost all Asian dust events observed in Korea contained considerable amounts of nitrate. However, Zhang et al. (2010a) reported an interesting result, i.e., the concentrations of $NO_3^-$ and $NH_4^+$ were lower during strong dust storm events than weak dust events. A high uncertainty appeared to exist for carrying amount of reactive nitrogen by dust particles.

A few contradictory results were also reported in the literature, which made the scientific issue even

more complicated. For example, the concentration of $NO_3^-$ in atmospheric aerosols on dust days was significantly lower in comparison to the concentration measured immediately before or after the event at a rural site in Yulin near the Asian dust source region (Wang et al., 2016b). The phenomenon was also observed in Shanghai, a mega city at a few thousands of kilometers from dust source zones in China, and more downwind sites (Kang et al., 2013; Li et al., 2014; Wang et al., 2013).

Inorganic nitrogen reportedly contributed to ~80% of the total water-soluble nitrogen (TDN) in atmospheric particles collected over the Yellow Sea and in Qingdao (Shi et al., 2012). In the region, the dry deposition flux of the inorganic nitrogen accounted for more than 75% for the TDN (Qi et al., 2013). When deposited to the ocean via atmospheric dry deposition, inorganic nitrogen has great impact on marine productivity due to its bioavailability. To update and improve our knowledge on reactive nitrogen carried by dust particles, we collected atmospheric aerosol particles during and prior to (or post, but only when no sample was collected prior to dust events) at a coastal site adjacent to the Yellow Sea in each spring of 2008-2011. The concentrations of $NO_2^-$, $NO_3^-$, $NH_4^+$ and other components were determined for analysis. In this study, we focused on nitrate and ammonium by excluding nitrite because of its very low concentration. We first characterized the concentrations of $NH_4^+$ and $NO_3^-$ in dust samples by comparing them with the values in atmospheric particles measured either prior to or post the event. We then conducted source apportionment to quantify their sources. Finally, we calculated and discussed the deposition flux of atmospheric particulate $NH_4^+$ and $NO_3^-$ during dust events.

## 2 Experimental methods

### 2.1 Sampling

Fig. 1 shows the sampling site, which is situated at the top of a coastal hill (Baguanshan) in Qingdao in northern China (36 ° 6' N, 120 ° 19' E, 77 m above sea level) and is approximately 1.0 km from the Yellow Sea to the east. A high-volume air sampler (Model KC-1000, Qingdao Laoshan Electronic Instrument Complex Co., Ltd., China) was set up on the roof of a two-story office building to collect total suspended particle (TSP) samples on quartz microfiber filters (Whatman QM-A) at a flow rate of 1 $m^3$/min. Prior to sampling, the filters were heated at 450 ℃ for 4.5 hrs to remove organic compounds. Our sample collection strategy involved collecting dust samples representing long-range transported

particles. We followed the definition of dust events adopted in the regulations of surface meteorological observations of China (CMA, 2004; Wang et al., 2008) and identified dust events based on the meteorological records (Weather Phenomenon) of Qingdao from the Meteorological Information Comprehensive Analysis and Process System (MICAPS) of the China Meteorological Administration. Due to no dust events lasting over 12 hrs (Lee et al., 2015; Su et al., 2017; Zhang et al., 2007), we collected one dust sample with a 4-hr duration in a day. The sampling for dust particles started only when the measured $PM_{10}$ mass concentration in Qingdao (http://www.qepb.gov.cn/m2/) and the forecasted dust mass over Asia (http://www-cfors.nies.go.jp/~cfors/) had greatly increased.

On March 20-21, 2010, two dust events subsequently swept Qingdao. The on-line data in high time-resolution can allow identifying two dust events accurately from the start to the end. The data confirmed that the 4 hr dust samples with IDs of 20100320 and 20100321 were well separated from each other for the two events, although they may not capture the entirety of the two events. The same was true for the dust samples with IDs of 20110501, 20110502. Table 1 lists the sampling information. Based on the forecast, we also collected aerosol particle samples immediately before, which were regarded as the reference samples. These reference samples were further classified into sunny day samples and cloudy day samples. For those events missing sampling prior to dust events, we collected post-dust samples under clear and sunny weather conditions as early as possible.

Asian dust events were mostly observed in the spring at the sampling site. Our intensive samplings were concentrated in the period of March to May in 2008-2011, when a smaller outbreak for Asian dust events was observed in northern China (Fig. S3). Overall, a total of 14 sets of dust samples and 8 sets of comparison samples were available for analysis in this study.

To facilitate the coastal sampling data analysis, sand samples were collected at the remote site of Zhurihe (42 °22'N, 112 °58'E) in the Hunshandake Desert, one of the main Chinese sand deserts, in April 2012. Sand samples were packed in clean plastic sample bags and were stored below -20 ℃ before the transfer. An ice-box was used to store the samples during transport to the lab for chemical analysis.

**2.2 Analysis**

The aerosol samples were weighted according to the standard protocol. The sample membranes were then cut into several portions for analysis. One portion of each aerosol sample was ultrasonically extracted with ultra-pure water in an ice water bath for determining inorganic water-soluble ions using

ICS-3000 ion chromatography (Qi et al., 2011). The sand samples collected at the Zhurihe site were analyzed using the same procedure.

One portion of each aerosol filter was cut into 60 $cm^2$ pieces and digested with $HNO_3$+$HClO_4$+HF (5:2:2 by volume) at 160 ℃ using an electric heating plate. The concentrations of Cu, Zn, Cr, Sc and Pb were measured using inductively coupled plasma mass spectrometry (Thermo X Series 2), while the concentrations of Al, Ca, Fe, Na and Mg were measured using inductively coupled plasma atomic emission spectroscopy (IRIS Intrepid II XSP). Field blank membranes were also analyzed for correction.

One portion of aerosol sample was digested with an $HNO_3$ solution (10% $HNO_3$, 1.6 M) at 160 ℃ for 20 min in a microwave digestion system (CEM, U.S.). The Hg and As in sample extracts were analyzed following the U.S. Environmental Protection Agency method 1631E (U.S. EPA, 2002) using cold vapor atomic fluorescence spectrometry (CVAFS). The detection limits, precisions and recoveries of water-soluble ions and metal elements are listed in Table 2.

### 2.3 Computational modeling

The enrichment factor of metal elements was given by

$$EF_i = \frac{\left(X_i / X_{\mathrm{Re}}\right)_{aerosols}}{\left(X_i / X_{\mathrm{Re}}\right)_{crust}} \quad (1)$$

where subscripts *i* and *Re* refer to the studied metal and the reference metal, respectively; $(X_i/X_{Re})_{aerosols}$ is the concentration ratio of metal *i* to metal *Re* in the aerosol samples; and $(X_i/X_{Re})_{crust}$ is the ratio of metal *i* to metal *Re* in the Earth's crust. For the calculation of the enrichment factor of the metal elements, scandium was used as the reference element (Han et al., 2012), and the abundance of elements in the Earth's crust given by Taylor (1964) was adopted.

The 72-h air mass back trajectories were calculated for each TSP sample using TrajStat software (Wang et al., 2009) and National Oceanic and Atmospheric Administration (NOAA) GDAS (Global Data Assimilation System) archive data (http:// www.arl.noaa.gov/ready/hysplit4.html). The air mass back trajectories were calculated at an altitude of 1500 m to identify the dust origin. In addition, the distance over sea of the air mass for each sample was measured from the trajectory using TrajStat software (Wang et al., 2009).

The positive matrix factorization (PMF) is a commonly used receptor modeling method. This model

can quantify the contribution of sources to samples based on the composition or fingerprints of the sources (Paatero and Tapper, 1993; Paatero, 1997). The measured composition data can be represented by a matrix X of *i* by *j* dimensions, in which *i* number of samples and *j* chemical species were measured, with uncertainty *u*. *X* can be factorized as a source profile matrix (*F*) with the number of source factors (*p*) and a contribution matrix (*G*) of each source factor to each individual sample, as shown in Equation 2.

$$X_{ij} = \sum_{k=1}^{p} G_{ik} F_{kj} + E_{ij} \quad (2)$$

where $E_{ij}$ is the residual for species *j* of the i-th sample.

The aim of the model is to minimize the objective function *Q*, which was calculated from the residual and uncertainty of all samples (Equation 3), to obtain the most optimal factor contributions and profiles.

$$Q = \sum_{i=1}^{n} \sum_{j=1}^{m} (E_{ij}/u_{ij})^2 \quad (3)$$

The EPA PMF 3.0 model was used to obtain the source apportionment of atmospheric particulates on dust and comparison days. Our modeled results satisfied the reasonable fit criteria, i.e. 90% of the scaled residuals were located between the range −3 and +3 for each species. The correlation coefficient between the predicted and observed concentrations was 0.97.

Dry deposition velocities were obtained using Williams' model (Williams, 1982) by accounting for particle growth (Qi et al., 2005). Williams' model is a two-layer model used to calculate the dry velocity of size-segregated particles over the water. In an upper layer below a reference height (10 m), the deposition of aerosol particles is governed by turbulent transfer and gravitational settling. In the deposition layer, the gravitational settling of particles is affected by particle growth due to high relative humidity. To obtain the deposition velocity of different particle sizes, Williams' model needs many input parameters, such as the wind speed at 10-m height ($U_{10}$), air/water temperature, and relative humidity. Relative humidity, air temperature and $U_{10}$ from the National Centers for Environmental Prediction (NCEP) were used in this study. Surface seawater temperature data was collected from the European Centre for Medium-Range Weather Forecasts (ECMWF). The meteorological and seawater temperature data had a six-hour resolution. According to a previously reported method (Qi et al., 2013), the dry deposition fluxes of the particles and the nitrogen species were calculated for dust and comparison days.

The CMAQ model (v5.0.2) was applied over the East Asia area to simulate the concentrations of

$PM_{10}$, $NO_x$ and $NH_3$ for 14 samples collected during 11 dust events. The simulated domain contains 164×97 grid cells with a 36-km spatial resolution, and the centered point was 110 °E, 34 °N. The vertical resolution includes 14 layers from the surface to the tropopause, with the first model layer at a height of 36 m above the ground level. The meteorological fields were generated by the Weather Research and Forecasting (WRF) Model (v3.7). Considering that the simulated area is connected to the Yellow Sea, the CB05Cl chemical mechanism was chosen to simulate the gas-phase chemistry. Zhang et al. (2009) generated the emissions of air pollutants in 2006 including $NO_X$ and $NH_3$ over East Asia and they updated the emission inventory in 2008 for us being used in this study. Initial conditions (ICONs) and boundary conditions were generated from a global chemistry model of GEOS-CHEM. All the dust events simulations are performed separately, each with a 1-week spin-up period to minimize the influence of the ICONs. The validation of the application of the CMAQ model in China has been reported by Liu et al. (2010a, b).

### 2.4 Other data sources and statistical analysis

Meteorological data were obtained from the Qingdao Meteorological Administration (http://qdqx.qingdao.gov.cn/zdz/ystj.aspx) and the MICAPS of the Meteorological Administration of China. Different weather characteristics, such as sunny days, cloudy days and dust days, were defined according to information from the MICAPS and Qingdao Meteorological Administration. According to the altitude, longitude and latitude of the 72-hr air mass back trajectory of each dust sample, the pressure level, temperature and relative humidity (RH) data along the path of the air mass were derived from the NCEP/NCAR re-analysis system (http://www.esrl.noaa.gov/psd/data/gridded/data.ncep.reanalysis.html) for each sample. The mixed layer depth during the air mass transport of dust samples was obtained from the HYSPLIT Trajectory Model (http://ready.arl.noaa.gov/hypub-bin/trajasrc.pl) using the same method. Then the average mixing layer, transport altitude, air temperature and RH were calculated as an average of all points on the air mass back trajectory of each sample. Spearman correlation analysis was applied to examine the relationships of nitrate and ammonium with transport parameters, and P values of $<0.05$ were considered to be statistically significant.

## 3 Results

### 3.1 Characterization of aerosol samples collected during dust events

We first examined the mass concentrations of TSP samples and the concentrations of crustal and anthropogenic metals therein through a comparison with the samples collected on dust days and reference samples on immediately before or after days, providing the background information for our target species analyzed later. The comparative results are highlighted below. For these reference samples, the TSP mass concentrations ranged from 94 to 275 $\mu g \cdot m^{-3}$, with an average of 201 $\mu g \cdot m^{-3}$ (Fig. 2, Table S1). The TSP mass concentration increased substantially to 410-3857 $\mu g \cdot m^{-3}$ in dust day samples, with an average of 1140 $\mu g \cdot m^{-3}$. In each individual pair of dust day sample against reference sample, a net increase in the mass concentration of TSPs was observed. The percentages varied from 82 to 1,303% on basis of events, with a mean value of 403% (Table S1). A similar increase was present in the crustal elements in each pair of samples. For example, the mean concentrations of Sc, Al, Fe, Mg and nss-Ca (usually used as a typical dust index) increased by more than a factor of two. On the other hand, the enrichment factors (EF) of Al, Fe, Ca, and Mg were less than three in dust day samples with values less than 14 in the reference samples (Table 3). Lower values are indicative of elements from a primarily crustal origin. The average mass concentrations of anthropogenic elements, such as Cu, Pb, Zn, Cr, Hg and As, in dust day samples increased by 107% to 722% against those in the reference sample; however, the EF of the anthropogenic metal elements decreased in the former. This indicates that dust particles likely carried more anthropogenic elements, although their relative contribution to the total mass was lower than that in the reference sample. Note that Sample 20110415 was excluded for further analysis. It was judged as a local blowing dust event because no corresponding dust event existed upwind.

### 3.2 Concentrations of $NH_4^+$ and $NO_3^-$ in dust day samples

When the mass concentrations of $NH_4^+$ and $NO_3^-$ in each pair of TSP samples were compared, the concentrations of $NH_4^+$ increased by 8%-473% in some dust day samples (20080301, 20080315, 20090316, 20100315, 20100320, 20100321, 20110418 and 20110502), but decreased by 28-84% in other dust day samples (Fig. 3, Column $NH_4^+$ and $NO_3^-$ in Table S1). The same was generally true for the measured concentrations of $NO_3^-$.

Considering the relative values of $NH_4^+$ and $NO_3^-$ in dust day samples relative to the reference samples, we classified the dust day samples into three categories (Table 4). In Category 1, the mass

concentrations of $NH_4^+$ and $NO_3^-$ were larger in dust day samples against the reference samples. In Category 2, the reverse was true. In Category 3, the mass concentrations of $NO_3^-$ were lower in the dust samples than in the reference samples, whereas the concentrations of $NH_4^+$ were close to the reference. As reported, the Yellow Sea encountered dust storms mainly derived from the Hunshandake Desert (Zhang and Gao, 2007). We thereby compared our observations with the sand particles collected from this desert (Table 5). The ratios of mass concentrations of nitrate and ammonium to the total mass of sand particles were very low, i.e., less than 81 μg/g, which are approximately three orders of magnitude less than the corresponding values in our dust samples. The values obtained from atmospheric aerosols at the urban sites of Duolun (Cui, 2009) and Alxa Right Banner (Niu and Zhang, 2000), which are closer to the desert, increased on dust days, but were still over one order of magnitude lower than the corresponding values in this study (Table 5). The mixing and chemical interaction between anthropogenic air pollutants and dust particles during transport from the source zone to the reception site likely played an important role in increasing the ratios, leading to extremely larger ratio values at this site relative to those in source dust and in upwind atmospheric particles (Cui et al., 2009; Wang et al., 2011; Wu et al., 2016). Since air pollutant emissions, meteorological conditions, chemical reactions, and others can affect the concentrations of $NH_4^+$ and $NO_3^-$ in atmospheric particles collected in dust days, the observed increase or decrease in the mass concentration of nitrate and ammonium in different dust samples against the reference implied the combined effect of those factors.

## 4. Discussion

### 4.1 Theoretical analysis of the three categories

Ammonium salts are common in atmospheric particles with diameters of less than 2 μm (Yao et al., 2003; Yao and Zhang, 2012). Many modeling studies have shown that the gas-aerosol thermodynamic equilibrium is assumed to be fully attained for inorganic ions, including ammonium salts in $PM_{2.5}$ (Dentener et al., 1996; Underwood et al., 2001; Wang et al., 2017a; Zhang et al., 1994; Zhang and Carmichael, 1999). Reasonably good agreements between ammonium salt modeling results and observations reported in the literature support the validity of this assumption (Chen et al., 2016; Penrodet al., 2014; Walker et al., 2012). Supposing that a thermodynamic equilibrium had been attained by the ammonium salts in Category 1, the reactions between carbonate salts and ammonium salts, such as 1) $(NH_4)_2SO_4 + CaCO_3 \Rightarrow CaSO_4 + NH_3$ (gas) $+CO_2$ (gas) $+H_2O$ and 2) $2NH_4NO_3+$

$CaCO_3 \Rightarrow Ca(NO_3)_2 + 2NH_3$ (gas) $+CO_2$ (gas) $+H_2O$, will release $NH_3$ (gas) until $CaCO_3$ has been completely used up. During dust events, very high concentrations of $Ca^{2+}$ were observed, and high $CaCO_3$ concentrations were therefore expected. For example, the single-particle characterization showed that Asia dust from the Gobi and Inner Mongolian Deserts had rich $CaCO_3$, with a ratio of 4.3-6.7% for reacted $CaCO_3$ and 3.0-4.6% for unreacted $CaCO_3$ (Hwang et al., 2008). Heterogeneous chemical reactions of mineral dust mostly occurred on $CaCO_3$ mineral dust (Hwang and Ro, 2006). However, when Category 1 was considered alone except for Sample 20100321, a good correlation was obtained for $[NH_4^+]_{\text{equivalent concentration}}=0.98*[NO_3^-+SO_4^{2-}]_{\text{equivalent concentration}}$ ($R^2=0.83$, $P<0.05$). The good correlation, together with the slope of 1, strongly indicated that the $NO_3^-$ and $SO_4^{2-}$ were almost completely associated with $NH_4^+$ in these dust day samples. Anthropogenic ammonium nitrate and ammonium sulfate were thought to be produced by gas, aqueous phase reaction and thermodynamic equilibrium processes and they usually internally mixed (Seinfeld and Pandis, 1998). In reverse, the poor correlation of $Ca^{2+}$ to $NO_3^-$ and $SO_4^{2-}$ showed that the formation of $CaSO_4$ and/or $Ca(NO_3)_2$ was probably negligible. Thus, ammonium salt aerosols very likely existed separately with dust aerosols in these dust day samples. Wang et al. (2017a) also found that coarse mode ammonium was quite low and fine mode dust particles existed separately with anthropogenic ammonium nitrate and ammonium sulfate. The observed $NO_3^-$ and $NH_4^+$ in Asia dust samples were argued due to physically mixing two types of particles rather than the heterogeneous formation of nitrate and ammonium (Huang et al., 2010). The hypothesis appeared to be valid in Category 1, where $NH_4^+$ was negatively correlated with $Ca^{2+}$ (Fig. S4). In the Sample 20100321 collected on 21 March 2010, $[NH_4^+]$ only accounted for ~70% of the observed $[NO_3^-+SO_4^{2-}]$ in an equivalent concentration. This result suggested that ~30% of ($NO_3^-+SO_4^{2-}$) may be associated with dust aerosols via the formation of metal salts of the two species. This hypothesis was supported by the correlation result, i.e., $NO_3^-$ was positively correlated with $NH_4^+$ and Cu, and $SO_4^{2-}$ was correlated with $K^+$, $Na^+$ and $Mg^{2+}$ (Fig. S4). Scheinhardt et al. (2013) found that $Cu^{2+}$ showed mixed organic and nitrate complexation in aerosol particles, using a thermodynamic model (E-AIM III). Cu was also detected to be partly in the form of nitrate in aerosol particles by single particle mass spectrometry (Wang et al., 2016a; Zhang et al., 2015). Cu was once used as an effective marker of diesel and biodiesel-blend exhaust (Gangwar et al., 2012), while it can also be derived from copper pyrites ($CuFeS_2$) in Inner Mongolia mines (Huang et al., 2010). The increase of Cu in the mass concentration in dust samples implied dust particles mixed with

anthropogenic particles, particularly from industrial emissions, during transport. In addition, many studies showed that $SO_4^{2-}$ can exist in many forms of metal salts in atmospheric particles, such as $Na_2SO_4$, $K_2SO_4$, $K_2Ca(SO_4)_2 \cdot H_2O$, $Na_2Ca(SO_4)_2$, $Na_2Mg(SO_4)_2 \cdot 4H_2O$, $(NH_4)_2Mg(SO_4)_2 \cdot 6H_2O$, $Na_3(NO_3)(SO_4) \cdot H_2O$ (Chabas and Lefèvre, 2000; Sobanska et al., 2012; Xie et al., 2005).

For Category 2, no correlation between $[NH_4^+]_{\text{equivalent concentration}}$ and $[NO_3^- + SO_4^{2-}]_{\text{equivalent concentration}}$ existed. When Category 2 was considered alone except for one Sample 20110501, the equivalent ratios of $NH_4^+$ to $NO_3^- + SO_4^{2-}$ were generally much smaller than 1, suggesting that a larger fraction of $NO_3^- + SO_4^{2-}$ may exist as metal salts due to reactions of their precursors with dust aerosols. $NO_3^-$ and $SO_4^{2-}$ showed no correlations with $NH_4^+$ but did show significant correlations with Pb (Fig. S4). The average concentration of $Ca^{2+}$ in Category 2 (0.43±0.40 μmol/m$^3$) was evidently higher than that in Category 1 ($Ca^{2+}$: 0.17±0.04 μmol/m$^3$), implying the probable formation of $CaSO_4$ and/or $Ca(NO_3)_2$ and the release of $NH_3$ (gas). Moreover, except for 20080502, the remaining dust samples in Category 2 were transported from the desert relatively enriched with $CaCO_3$ (1-25% in Wt%) (Formenti et al., 2011). A positive correlation between $NO_3^-$ and $SO_4^{2-}$ in Category 2 against a negative correlation in Category 1 also implied that the dust particles enriched with $CaCO_3$ in Category 2 might play an important role to form $SO_4^{2-}$ and $NO_3^-$. Ca-rich dust particles coated with highly soluble nitrate were observed at Kanazawa in Japan during Asian dust storm periods using SEM/EDX (scanning electron microscopy equipped with an energy dispersive X-ray spectrometer) (Tobo et al., 2010). The single-particle observation conducted by Hwang and Ro (2006) showed that $CaCO_3$ in dust particles was almost completely consumed to produce mainly $Ca(NO_3)_2$ species.

There were only three samples in Category 3. $[NH_4^+]_{\text{equivalent concentration}} = 0.95 * [NO_3^- + SO_4^{2-} + Cl^-]_{\text{equivalent concentration}}$ was obtained for Sample 20110418, implying that the $NH_4^+$ was not only associated with $NO_3^-$ and $SO_4^{2-}$ but also with $Cl^-$. In the sample collected on 15 March 2010, $[NH_4^+]$ accounted for 78% of the observed $[NO_3^- + SO_4^{2-}]$ in an equivalent concentration. As discussed above, ~20% of $(NO_3^- + SO_4^{2-})$ may be associated with dust aerosols via the formation of metal salts of the two species. The equivalent ratio of $NH_4^+$ to $NO_3^- + SO_4^{2-}$ was only 0.14 for Sample 20100320, and $Ca^{2+}$ for this sample (0.47 μmol/m$^3$) was evidently higher than that for Sample 20100315 ($Ca^{2+}$: 0.12 μmol/m$^3$) and 20110418 ($Ca^{2+}$: 0.12 μmol/m$^3$), suggesting that a larger fraction of $NO_3^- + SO_4^{2-}$ may exist as metal salts. However, the unique changes in $NH_4^+$ and $NO_3^-$, different from Category 1 and 2, need further

investigation.

### 4.2 Source apportionment of aerosols during dust and non-dust events

The sources of atmospheric aerosols in dust and reference samples were determined by PMF modeling (Paatero and Tapper, 1993; Paatero, 1997). Fig. 4 shows that atmospheric aerosols in the reference samples mainly included six sources, i.e., industry, soil dust, secondary aerosols, sea salt, biomass burning, and coal combustion/other sources. In these dust samples, including Categories 1-3, oil combustion, industry, soil dust, secondary aerosols, and coal combustion/other sources were identified as five major sources (Table 6). The contribution of soil dust evidently increased from 23% to 36% in the dust samples relative to the reference, consistent with the high concentrations of TSPs and crustal metals observed on dust days. The calculated contribution of nitrate plus ammonium from the soil dust source to the total mass of nitrate plus ammonium in the dust samples greatly increased. The source profile for coal combustion in the dust day samples showed a high percentage of $K^+$, $Cl^-$, Ca, Mg, Co, Ni, As, Al and Fe, indicating that coal combustion particles may exist contemporaneously with other anthropogenic pollutants emitted along the transport path. Liu et al. (2014) also found a larger net increase in the contribution of dust aerosols to the mass of $PM_{10}$, i.e., 31%-40%, on dust days against non-dust days in Beijing which is approximately 600 km upwind of Qingdao. Accordingly, they reported that the contributions of local anthropogenic sources decreased on dust days, especially those from secondary aerosols, consistent with the EF of anthropogenic metals observed on dust days.

### 4.3 Influence of transport path ways on $NH_4^+$ and $NO_3^-$ in dust samples

The calculated air mass trajectories for 13 out of 14 samples showed that the air mass originated from North and Inner Mongolia, China (Fig. 5), generally consistent with the results of Zhang and Gao (2007). The remaining one, with ID of 20110418 originated from Northeast China. The calculated trajectories showed that the entire dust air mass passed over those highly polluted regions with strong modeled emissions of $NO_x$ and $NH_3$ shown in Fig 6 and experienced different residence times therein. Fig. 5 shows that all air mass trajectories in Category 1 were transported from either the north or northwest over the continent, except for the Sample 20110502. In Category 2, the air masses always took a 94-255 km trip over the sea prior to arriving at the reception site. $NH_3$-poor conditions in the marine atmosphere disfavored the formation and existence of ammonium nitrate. On the other hand,

the humid marine conditions (the calculated average RH ranged in 50-75% over the Bohai and Yellow Seas in 2006-2012 using NCEP/NCAR re-analysis data) might have enhanced hetero-coagulation between dust and smaller anthropogenic particles, leading to the release of $NH_3$ via reactions between preexisting ammonium salts and carbonate salts.

The average mixing layer was less than 900 m along the air mass transport routes for most sampling days in Category 1 (Table 7), favoring the trapping of locally emitted anthropogenic air pollutants in the mixing layer. The air masses in Category 1 took over 11-39 hrs to cross over the highly polluted area with appreciable modeled concentrations of $NO_x$ (5.7±1.4 ppb) and $NH_3$ (7.6±3.3 ppb). Except for two samples (ID of 20080529 and 20110319), air masses in Category 2 took less than 10 hrs to cross over the polluted areas with lower concentrations of $NO_x$ (modeled value: 3.6±3.4 ppb) and $NH_3$ (modeled value: 4.7±4.7 ppb) and the mixing layer height along the route was 916-1194 m (on average) for each dust event. Moreover, the averaged wind speed at sampling site was 2.8 m/s in Category 1, but 6.2 m/s in Category 2. The lower wind speed in Category 1 was unexpected, implying dust particles very likely traveled at aloft with a high speed and then mixed down to the ground through subsidence. This further led to the external mixing of anthropogenic particulate matters and dust. The correlation analysis results in Table S2 indirectly support these conclusions.

The concentrations of $PM_{10}$ and its major components $NO_3^-$ and $NH_4^+$ over East Asia on dust days and comparison days were modeled using the WRF-CMAQ model (Fig. S5-6). Spatial distributions of simulated $PM_{10}$ during each dust events were consistent with the records in the "Sand-dust Weather Almanac" (CMA, 2009; 2010; 2012; 2013). The dust particles were transported eastward by passing over the sampling site, the China Sea and arriving at the far remote ocean region, except for the local blowing dust sample with ID of 20110415, as mentioned previously. NMB (normalized mean bias) values of simulated $NO_3^-$ were -4% and -12% in dust and non-dust reference samples, respectively, indicating that CMAQ results reasonably reproduce the mass concentrations of $NO_3^-$ (Fig. S6). Simulated $NH_4^+$ concentrations in dust samples were severely under-predicted with NMB values at -71%. For reference samples, simulated $NH_4^+$ concentrations sometimes can well reproduce the observational values, but the simulation was sometimes severely deviated from the observation. The deviation could be related to many factors which were out of scope of this study. The separately mixing mechanism proposed in this study is urgently needed to be included in the model for accurately predicting the concentrations during dust events.

### 4.4 Dry deposition fluxes of TSP, $NH_4^+$, $NO_3^-$ and metals

Dust events are known to increase the deposition fluxes of aerosol particles along the transport path because of high particle loadings. For example, Fu et al. (2014) found that the long-range transported dust particles increased the dry deposition of $PM_{10}$ in the Yangtze River Delta region by a factor of approximately 20. In terms of atmospheric deposition in the oceans, a few studies reported enhancements in oceanic chlorophyll *a* following dust storm events (Banerjee and Kumar, 2014; Tan and Wang, 2014). In addition to those in high-nutrient and low-chlorophyll (HNLC) regions, the input of nitrogen and other nutrients associated with dust deposition is expected to promote the growth of phytoplankton in oceans with varying nutrient limitation conditions. Thus, we calculated the dry deposition fluxes of aerosols particles, $N_{NH4+NO3-}$ and metal elements during dust and reference periods using the measured component concentrations and modeled dry deposition velocities (Table 8). We also compared the calculated dry deposition flux of TSP and $N_{NH4+NO3}$- with previous observations in the literature.

The calculated dry deposition fluxes of atmospheric particulates increased on dust days against the reference to some extent. For example, the particle deposition fluxes varied over a wide range from 5,200 to 65,000 mg/m$^2$/month in different dust sampling days, with an average of 18,453 mg/m$^2$/month, in comparison with the dry deposition flux of TSP of 2,800±700 mg/m$^2$/month from the reference periods in the coastal region of the Yellow Sea. The dry deposition fluxes of $N_{NH4+NO3}$- varied, depending on Category 1, 2 or 3. In Category 1, the dry deposition fluxes of $N_{NH4+NO3}$- increased by 9-75% with increased TSP flux by 86-252% (Table S3). In Categories 2 and 3, the dry deposition fluxes of TSP increased by 126% to 2,226% against the references. The dry deposition fluxes of particulate $N_{NH4+NO3}$- decreased by 50%, on average, in Categories 2 and 3, although the fluxes of ammonium of two samples in Category 3 increased. A larger decrease against the reference in the flux of nitrate was present in Categories 2 and 3, i.e., decreases of 73% and 46%, respectively. The ammonium deposition flux also decreased by 47% in Category 2 but increased by 10% in Category 3.

Except for Pb and Zn in Category 2, the calculated dry deposition fluxes of Cu, Pb and Zn increased with those of nitrogen on dust days. Trace metals were found to have a toxic effect on marine phytoplankton and inhibit their growth (Bielmyer et al., 2006; Echeveste et al., 2012). Liu et al. (2013) found that inhibition coexisted with the promotion of phytoplankton species in incubation experiments

in the southern Yellow Sea in the spring of 2011 by adding Asian dust samples to collected seawater. However, the calculated dry atmospheric deposition fluxes of Fe increased by a factor of 124-2,370% in dust day samples. Wang et al. (2017b) recently reported that Fe can alleviate the toxicity of heavy metals. Moreover, atmospheric inputs of iron to the ocean have been widely proposed to enhance primary production in HNLC areas (Jickells et al., 2005).

Due to anthropogenic activity and economic development, $NO_x$ and $NH_3$ emissions were reported to increase in China from 1980 to 2010 (Fig. S3; Liu et al., 2017). The dry deposition flux of $N_{NH4+NO3}$- should have theoretically increased with the increase in the emission of inorganic nitrogen. Considering the different dry deposition velocities to be used in various studies, we recalculated the dry deposition flux of $N_{NH4+NO3}$- in the literature using the dry deposition velocities of 1 cm/s for nitrate and 0.1 m/s for ammonium, as reported by Duce et al. (1991). We thereby found that dry deposition fluxes of $N_{NH4+NO3}$- over the Yellow Sea during the dust days increased greatly from 1999 to 2007, but the values in Qingdao varied narrowly within a range of 94.75-99.65 mg N/$m^2$/month during the dust days from 1997 to 2011 (Table 9). The complicated results implied that even more updated works are needed in the future.

## 5 Conclusion

The concentrations of nitrate and ammonium in TSP samples varied greatly from event to event on dust days. Relative to the reference samples, the concentrations were both higher in some cases and lower in others. The observed ammonium in dust day samples was explained by $NH_4^+$ was likely either in the form of ammonium salts existing separately with dust aerosols or as the residual of incomplete reactions between ammonium salts and carbonate salts. $NO_3^-$ in the dust day samples can be due to either mixing or reactions between anthropogenic air pollutants and dust particles or combined both during the transport from the source zone to the reception site. However, this process was generally much less effective and led to a sharp decrease in nitrate in TSP samples of Category 2. The existence of ammonium salt aerosols separately with dust aerosols and the extent of the reactions between ammonium salts and carbonate salts were apparently associated with the transport pathway, metrological conditions and precursor emissions, and other factors. Due to a sharp increase in dust loads on dust days, the contribution of dust to the total aerosol mass increased against the samples

collected on other days. The contributions from local anthropogenic sources were accordingly lower on dust days.

Overall, this study strongly suggested that atmospheric deposition of $N_{NH4+NO3-}$ on dust days varied greatly. A simple assumption of a linear increase in $N_{NH4+NO3-}$ with increasing dust load, like that in the literature, could lead to a considerable overestimation of the dry deposition flux of nutrients into the oceans and the consequent primary production associated with dust events.

***Acknowledgments.*** This work was supported by the Department of Science and Technology of the P. R. China through the State Key Basic Research & Development Program under Grant No. 2014CB953701 and the National Natural Science Foundation of China (No. 41375143). We thank Prof. Yaqiang Wang and Jinhui Shi for the valuable discussion regarding this research. We also express our appreciation to Tianran Zhang for help with sand sampling, and Qiang Zhang, Yang Yu and Jiuren Lin for data collection.

## References

Banerjee, P., and Kumar, P. S.: Dust-induced episodic phytoplankton blooms in the Arabian Sea during winter monsoon, J. Geophys. Res-Oceans., 119, 7123-7138, 2014.

Bielmyer, G. K., Grosell, M., and Brix, K. V.: Toxicity of silver, zinc, copper, and nickel to the copepod Acartia tonsa exposed via a phytoplankton diet, Environ. Sci. technol., 40, 2063-2068, 2006.

Chabas, A., and Lefèvre, R. A.: Chemistry and microscopy of atmospheric particulates at Delos (Cyclades–Greece), Atmos. Environ., 34, 225–238, 2000.

Chen, D., Liu, Z. Q., Fast, J., and Ban, J. M.: Simulations of sulfate–nitrate–ammonium (SNA) aerosols during the extreme haze events over northern china in october 2014, Atmos. Chem. Phys., 16, 10707-10724, 2016.

CMA: Regulations of Surface Meteorological Observation, China Meteorological Press, Beijing, 154–156, 2004.

CMA: Sand-dust weather almanac 2008, China Meteorological Press, Beijing, 10-64, 2009.

CMA: Sand-dust weather almanac 2009, China Meteorological Press, Beijing, 11-59, 2010.

CMA: Sand-dust weather almanac 2010, China Meteorological Press, Beijing, 11-79, 2012.

CMA: Sand-dust weather almanac 2011, China Meteorological Press, Beijing, 10-53, 2013.

Creamean, J. M., Suski, K. J., Rosenfeld, D., Cazorla, A., DeMott, P. J., Sullivan, R. C., White, A. B., Ralph, F. M., Minnis, P., Comstock, J. M., Tomlinson, J. M., Prather, K. A.: Dust and Biological Aerosols from the Sahara and Asia Influence Precipitation in the Western U.S., Science, 339, 1572-1578, 2013.

Cui, W. L.: Chemical transformation of dust components and mixing mechanisms of dust with pollution aerosols during the long range transport from north to south China, M.S. thesis, Department of Environmental Science and Engineering, Fudan University, China, 38 pp., 2009.

Dai, Y.J.: Vertical distribution of characteristics of dust aerosols in the near-surface in hinterland of

Taklimakan Desert, M.S. thesis, College of Resources and Environmental Science, Xinjiang University, China, 26 pp., 2016.

Dentener, F. J., Carmichael, G. R., Zhang, Y., Lelieveld, J., and Crutzen, P. J.: Role of mineral aerosol as a reactive surface in the global troposphere, J. Geophys. Res-Atmos., 101, 22869-22889, 1996.

Duce, R. A., LaRoche, J.,Altieri, K., Arrigo, K. R., Baker, A. R., Capone, D. G., Cornell, S., Dentener, F., Galloway, J., Ganeshram, R. S., Geider, R. J., Jickells, T., Kuypers, M. M., Langlois, R., Liss, P. S., Liu, S. M., Middelburg, J. J., Moore, C. M., Nickovic, S., Oschlies, A., Pedersen, T., Prospero, J., Schlitzer, R., Seitzinger, S., Sorensen, L. L., Uematsu, M., Ulloa, O., Voss, M., Ward, B., and Zamora, L.: Impacts of atmospheric anthropogenic nitrogen on the open ocean, Science, 320, 893-897, 2008.

Duce, R. A., Liss, P. S., Merrill, J. T., Atlas, E. L., Buat-Menard, P., Hicks, B. B., Miller, J. M., Prospero, J. M., Arimoto, R., Church, T. M., Ellis, W., Galloway, J. N., Hansen, L., Jickells, T. D., Knap, A. H., Reinhardt, K. H., Schneider, B., Soudine, A., Tokos, J. J., Tsunogai, S., Wollast, R., and Zhou, M. Y.: The atmospheric input of trace species to the world ocean, Global. Biogeochem. Cy., 5, 193-259, 1991.

Echeveste, P., Agustí, S., and Tovar-Sánchez, A.: Toxic thresholds of cadmium and lead to oceanic phytoplankton: cell size and ocean basin-dependent effects, Environ. Toxicol. Chem., 31, 1887-1894, 2012.

Fitzgerald, E., Ault, A. P., Zauscher, M. D., Mayol-Bracero, O. L., and Prather, K. A.: Comparison of the mixing state of long-range transported Asian and African mineral dust, Atmos. Environ., 115, 19-25, 2015.

Formenti, P., Schütz's, L., Balkanski, Y., Desboeufs, K., Ebert, M., Kandler, K., Petzold, A., Scheuvens, D., Weinbruch, S., and Zhang, D.: Recent progress in understanding physical and chemical properties of African and Asian mineral dust, Atmos. Chem. Phys., 11, 8231–8256, 2011.

Fu, X., Wang, S. X., Cheng, Z., Xing, J., Zhao, B., Wang, J. D., and Hao, J. M.: Source, transport and impacts of a heavy dust event in the Yangtze River Delta, China, in 2011, Atmos. Chem. Phys., 14, 1239-1254, 2014.

Gangwar, J. N., Gupta, T., and Agarwal, A.K.: Composition and comparative toxicity of particulate matter emitted from a diesel and biodiesel fuelled CRDI engine, Atmos. Environ., 46, 472-481, 2012.

Grice, S., Stedman, J., Kent, A., Hobson, M., Norris, J., Abbott, J., and Cooke, S.: Recent trends and projections of primary $NO_2$ emissions in Europe, Atmos. Environ., 43, 2154-2167, 2009.

Guo, C., Yu, J., Ho, T. Y., Wang, L., Song, S., Kong, L., and Liu, H.: Dynamics of phytoplankton community structure in the South China Sea in response to the East Asian aerosol input, Biogeosciences, 9, 1519-1536, 2012.

Han, X., Ge, C., Tao, J. H., Zhang, M. G., and Zhang, R. J.: Air quality modeling for of a strong dust event in east Asia in march 2010, Aerosol. Air. Qual. Res., 12, 615-628, 2012.

Huang, K., Zhuang, G., Li, J., Wang, Q., Sun, Y., Lin Y., and Fu J. S.: Mixing of Asian dust with pollution aerosol and the transformation of aerosol components during the dust storm over China in spring 2007, J. Geophys. Res-Atmos, 115, D00k13, Doi:10.1029/2009jd013145, 2010.

Hwang, H. and Ro, C. U.: Direct observation of nitrate and sulfate formations from mineral dust and sea-salts using low-Z particle electron probe X-ray microanalysis, Atmos. Environ., 40, 3869-3880, 2006.

Hwang, H., Kim, H. K., and Ro, C. U.: Single-particle characterization of aerosol samples collected

515 before and during an Asian dust storm in Chuncheon, Korea, Atmos. Environ., 42, 8738–8746, 2008.
516 Jickells, T. D., An, Z. S., Andersen, K. K., Baker, A. R., Bergametti, G., Brooks, N., Cao, J. J., Boyd, P.
517 W., Duce, R. A., Hunter, K., Kawahata, H., Kubilay, N., laRoche, J.,Liss, P. S., Mahowald, N.,
518 Prospero, J. M., Ridgwell, A. J., Tegen, I., and Torres, R.: Global iron connections between desert
519 dust, ocean biogeochemistry, and climate, Science, 308, 67-71, 2005.
520 Kang, E., Han, J., Lee, M., Lee, G., and Kim, J. C.: Chemical characteristics of size-resolved aerosols
521 from Asian dust and haze episode in Seoul Metropolitan City, Atmos. Res., 127, 34-46, 2013.
522 Lee, Y. G., Ho, C., Kim, J., and Kim, J.: Quiescence of Asian dust events in South Korea and Japan
523 during 2012 spring: Dust outbreaks and transports, Atmos. Environ., 114, 92-101, 2015.
524 Li, W. J., Shao, L. Y., Shi, Z. B., Chen, J. M., Yang, L. X., Yuan, Q., Yan, C., Zhang, X. Y., Wang, Y. Q.,
525 Sun, J. Y., Zhang, Y, M., Shen, X. J., Wang, Z. F., and Wang, W. X.: Mixing state and hygroscopicity
526 of dust and haze particles before leaving Asian continent, J. Geophys. Res-Atmos., 119, 1044–1059,
527 2014.
528 Lin, X. H., Liu, C. L., and Zhang, H.: Determination of Metal Elements in Aerosol by ICP-AES, Rock
529 & Mineral Analysis, 17, 143-146, 1998.
530 Liu, L., Zhang, X. Y., Xu, W., Liu, X. J., Li, Y., Lu, X. H., Zhang, Y. H., and Zhang, W. T.: Temporal
531 characteristics of atmospheric ammonia and nitrogen dioxide over China based on emission data,
532 satellite observations and atmospheric transport modeling since 1980, Atmos. Chem. Phys., 106,
533 1-32, 2017.
534 Liu, Q. Y., and Bei, Y. L.: Impacts of crystal metal on secondary aliphatic amine aerosol formation
535 during dust storm episodes in Beijing, Atmos. Environ., 128, 227-334, 2016.
536 Liu, Q. Y., Liu, Y. J., Yin, J. X., Zhang, M. G., and Zhang, T. T.: Chemical characteristics and source
537 apportionment of PM10 during Asian dust storm and non-dust storm days in Beijing, Atmos.
538 Environ., 91, 85-94, 2014.
539 Liu, X. H., Zhang, Y., Cheng, S. H., Xing, J., Zhang, Q., Streets, D. G., Jang, C., Wang, W. X., and Hao,
540 J. M.: Understanding of regional air pollution over China using CMAQ, part I performance
541 evaluation and seasonal variation, Atmos. Environ., 44, 2415-2426, 2010a.
542 Liu, X. H., Zhang, Y., Xing, J., Zhang, Q., Wang, K., Streets, D. G., Jang, C., Wang, W. X., and Hao, J.
543 M.: Understanding of regional air pollution over China using CMAQ, part II. Process analysis and
544 sensitivity of ozone and particulate matter to precursor emissions, Atmos. Environ., 44, 3719-3727,
545 2010b.
546 Liu, Y., Zhang, T. R., Shi, J. H., Gao, H. W., and Yao, X. H.: Responses of chlorophyll a to added
547 nutrients, Asian dust, and rainwater in an oligotrophic zone of the Yellow Sea: Implications for
548 promotion and inhibition effects in an incubation experiment, J. Geophys. Res-Biogeo., 118,
549 1763-1772, 2013.
550 Ma, Q. X., Liu, Y. C., Liu, C., Ma, J. Z., and He, H.: A case study of Asian dust storm particles:
551 Chemical composition, reactivity to $SO_2$ and hygroscopic properties, J. Environ. Sci., 24, 62-71,
552 2012.
553 Mori, I., Nishikawa, M., Tanimura, T., and Quan, H.: Change in size distribution and chemical
554 composition of kosa (Asian dust) aerosol during long-range transport, Atmos. Environ., 37,
555 4253-4263, 2003.
556 Niu, S. J., and Zhang, C. C.: Researches on sand aerosol chemical composition and enrichment factor
557 in the spring at Helan Mountain area, Journal of Desert Research, 20, 264-268, 2000.
558 Ohara, T., Akimoto, H., Kurokawa, J., Horii, N., Yamaji, K., Yan, X., and Hayasaka, T.: An Asian

559 emission inventory of anthropogenic emission sources for the period 1980-2020, Atmos. Chem.
560 Phys., 7, 4419-4444, 2007.
561 Paatero, P., and Tapper, U.: Analysis of different modes of factor analysis as least squares fit problems,
562 Chemometr. Intell. Lab., 18, 183-194, 1993.
563 Paatero, P.: Least squares formulation of robust non-negative factor analysis, Chemometr. Intell. Lab.,
564 37, 23-35, 1997.
565 Penrod, A., Zhang, Y., Wang, K., Wu, S. Y. and Leung, L. R.: Impacts of future climate and emission
566 changes on U.S. air quality, Atmos. Environ., 89, 533-547, 2014.
567 Qi, J. H., Gao, H. W., Yu, L. M., and Qiao, J. J.: Distribution of inorganic nitrogen-containing species
568 in atmospheric particles from an island in the Yellow Sea, Atmos. Res., 101, 938-955, 2011.
569 Qi, J. H., Li, P. L., Li, X. G., Feng, L. J., and Zhang, M. P.: Estimation of dry deposition fluxes of
570 particulate species to the water surface in the Qingdao area, using a model and surrogate surfaces,
571 Atmos. Environ., 39, 2081-2088, 2005.
572 Qi, J. H., Shi, J. H., Gao, H. W., and Sun, Z.: Atmospheric dry and wet deposition of nitrogen species
573 and its implication for primary productivity in coastal region of the Yellow Sea, China, Atmos.
574 Environ., 81, 600-608, 2013.
575 Scheinhardt, S., Müller, K., Spindler, G., and Herrmann, H.: Complexation of trace metals in
576 size-segregated aerosol particles at nine sites in Germany, Atmos. Environ.,74,102-109, 2013.
577 Seinfeld, J. H., and Pandis, S. N.: Atmospheric Chemistry and Physics: From Air Pollution to Climate
578 Change, 2nd Edition, Wiley, New York, 1191 pp., 1998.
579 Sheng, Y., Yang, S., Han, Y., Zheng, Q., and Fang, X.: The concentrations and sources of nitrate in
580 aerosol over Dolmud, Qinghai, China, Journal of Desert Research, 36, 792-797, 2016.
581 Shi, J. H., Gao, H. W., Zhang, J., Tan, S. C., Ren, J. L., Liu, C. G., Liu, Y., and Yao, X. H.: Examination
582 of causative link between a spring bloom and dry/wet deposition of Asian dust in the Yellow Sea,
583 China, J. Geophys. Res-Atmos., 117, 127-135, 2012.
584 Shi, J. H., Zhang, J., Gao, H. W., Tan, S. C., Yao, X. H., and Ren, J. L.: Concentration, solubility and
585 deposition flux of atmospheric particulate nutrients over the Yellow Sea, Deep-sea. Res. Pt. II, 97,
586 43-50, 2013.
587 Skjøth C. A., and Hertel, O.: Ammonia Emissions in Europe, in Urban Air Quality in Europe,
588 Springer Berlin Heidelberg, Germany, 141-164, 2013.
589 Sobanska, S., Hwang, H., Choël, M., Jung, H., Eom, H., Kim, H., Barbillat, J., and Ro C.: Investigation
590 of the Chemical Mixing State of Individual Asian Dust Particles by the Combined Use of Electron
591 Probe X-ray Microanalysis and Raman Microspectrometry, Anal. Chem., 84 (7), 3145–3154, 2012.
592 Su, X., Wang, Q., Li, Z., Calvello, M., Esposito, F., Pavese, G., Lin, M., Cao, J., Zhou, C., Li, D., and
593 Xu, H.: Regional transport of anthropogenic pollution and dust aerosols in spring to Tianjin — A
594 coastal megacity in China, Sci. Total. Environ., 584-585, 381-392, 2017.
595 Tan, S. C., and Wang, H.: The transport and deposition of dust and its impact on phytoplankton growth
596 in the Yellow Sea, Atmos. Environ., 99, 491-499, 2014.
597 Taylor, S. R.: Abundance of chemical elements in the continental crust: a new table, Geochim.
598 Cosmochim. Ac., 28, 1273-1285, 1964.
599 Tobo, Y., Zhang, D. Z., Matsuki, A., and Iwasaka, Y.: Asian dust particles converted into aqueous
600 droplets under remote marine atmospheric conditions, PNAS Proceedings of the National Academy
601 of Sciences of the United States of America, 107, 17905–17910, 2010.
602 U. S., EPA.: Method 1631, Revision E: Mercury in water by oxidation, purge and trap, and cold vapor

atomic fluorescence spectrometry, US Environmental Protection Agency Washington, DC, 2002.
Underwood, G. M., Song, C. H., Phadnis, M., Carmichael, G. R., and Grassian, V. H.: Heterogeneous reactions of $NO_2$ and $HNO_3$ on oxides and mineral dust: a combined laboratory and modeling study, J. Geophys. Res-Atmos., 106, 18055-18066, 2001.
Uno, I., Eguchi, K., Yumimoto, K., Takemura, T., Shimizu, A., Uematsu, M., Liu, Z., Wang, Z., Hara, Y., and Sugimoto, N.: Asian dust transported one full circuit around the globe, Nat. Geosci., 2, 557-560, 2009.
VanCuren, R., and Cahill, T.: Asian aerosols in North America: Frequency and concentration of fine dust, J. Geophys. Res., 107(D24), 4804, doi:10.1029/2002JD002204, 2002.
Walker, J. M., Philip, S., Martin, R. V., and Seinfeld, J. H.: Simulation of nitrate, sulfate, and ammonium aerosols over the United States, Atmos. Chem. Phys., 12, 11213-11227, 2012.
Wang, F. J., Chen, Y., Guo, Z. G., Gao, H. W., Mackey, K. R., Yao, X. H., Zhuang, G. S. and Paytan, A.: Combined effects of iron and copper from atmospheric dry deposition on ocean productivity, Geophys. Res. Lett., 44, 2546-2555, 2017b.
Wang, H., An, J., Shen, L., Zhu, B., Xia, L., Duan, Q., and Zou, J.: Mixing state of ambient aerosols in Nanjing city by single particle mass spectrometry, Atmos. Environ., 132, 123-132, 2016a.
Wang, L., Du, H. H., Chen, J. M., Zhang, M., Huang, X. Y., Tan, H. B., Kong, L. D., and Geng, F. H.: Consecutive transport of anthropogenic air masses and dust storm plume: Two case events at Shanghai, China, Atmos. Res., 127, 22-33, 2013.
Wang, Q. Z., Zhuang, G. S., Huang, K., Liu, T. N., Lin, Y. F., Deng, C. R., Fu, Q. Y., Fu, J. S., Chen, J. K., Zhang, W. J., and Yiming, M.: Evolution of particulate sulfate and nitrate along the Asian dust pathway: Secondary transformation and primary pollutants via long-range transport, Atmos. Res., 169, 86-95, 2016b.
Wang, Q. Z., Zhuang, G. S., Li, J., Huang, K., Zhang, R., Jiang, Y. L., Lin, Y. F., and Fu, J. S.: Mixing of dust with pollution on the transport path of Asian dust - Revealed from the aerosol over Yulin, the north edge of Loess Plateau, Sci. Total. Environ., 409, 573-581, 2011.
Wang, Y. Q., Zhang, X. Y., and Draxler, R. R.: TrajStat: GIS-based software that uses various trajectory statistical analysis methods to identify potential sources from long-term air pollution measurement data, Environ. Modell. Softw., 24, 938-939, 2009.
Wang, Y. Q., Zhang, X. Y., Gong, S. L., Zhou, C. H., Hu, X. Q., Liu, H. L., Niu, T., and Yang, Y. Q.: Surface observation of sand and dust storm in East Asia and its application in CUACE/Dust, Atmos. Chem. Phys., 8, 545-553, 2008.
Wang, Z., Pan, X., Uno, I., Li, J., Wang, Z., Chen, X., Fu, P., Yang, T., Kobayashi, H., Shimizu, A., Sugimoto, N., and Yamamoto, S.: Significant impacts of heterogeneous reactions on the chemical composition and mixing state of dust particles: A case study during dust events over northern China, Atmos. Environ., 159, 83-91, 2017a.
Williams, R. W.: A model for the dry deposition of particles to natural water surface, Atmos. Environ., 16, 1933-1938, 1982.
Wu, F., Zhang, D. Z., Cao, J. J., Guo, X., Xia, Y., Zhang, T., Lu, H., and Cheng, Y.: Limited production of sulfate and nitrate on front-associated dust storm particles moving from desert to distant populated areas in northwestern China, Atmos. Chem. Phys., 853, 1-22, 2016.
Xie, R. K., Seip, H. M., Leinum, J. R., Winje, T., and Xiao, J. S.: Chemical characterization of, individual particles (PM10) from ambient air in Guiyang City, Sci. Total. Environ., 343(1-3).261-271, 2005.

Xin, W. C., Lin, X. H., and Xu, L.: ICP-MS Determination of 34 trace elements in marine sediments, Physical Testing and Chemical Analysis (Part B: Chemical Analysis), 4, 29, 2012.

Xu, J. Z., Wang, Z. B., Yu, G. M., Qin, X., Ren, J. W., and Qin, D. H.: Characteristics of water soluble ionic species in fine particles from a high altitude site on the northern boundary of Tibetan Plateau: Mixture of mineral dust and anthropogenic aerosol, Atmos. Res., 143, 43-56, 2014.

Yang, D. Z., Wang, C., Wen, Y. P., Yu, X. L., and Xiu, X. B.: Analysis of Two Sand Storms In Spring 1990, Quarterly Journal of Applied Meteorology, 6, 18-26, 1995.

Yang, D. Z., Yan, P., and Xu, X. D.: Characteristics of aerosols under dust and sand weather in Beijing, Quarterly Journal of Applied Meteorology, 1, 185-194, 2002.

Yao, X. H., and Zhang, L.: Supermicron modes of ammonium ions related to fog in rural atmosphere, Atmos. Chem. Phys., 12, 11165-11178, 2012.

Yao, X. H., Lau, A. S., Fang, M., Chan, C., and Hu, M.: Size Distributions and Formation of Ionic Species in Atmospheric Particulate Pollutants in Beijing, China: 1—Inorganic Ions. Atmos. Environ., 37, 2991-3000, 2003.

Zhang, G. S., Zhang, J., and Liu, S. M.: Characterization of nutrients in the atmospheric wet and dry deposition observed at the two monitoring sites over Yellow Sea and East China Sea, J. Atmos. Chem., 57, 42-57, 2007.

Zhang, G., Han, B., Bi, X., Dai, S., Huang, W., Chen, D., Wang, X., Sheng, G., Fu, J., and Zhou, Z.: Characteristics of individual particles in the atmosphere of Guangzhou by single particle mass spectrometry, Atmos. Res., 153, 286-295, 2015.

Zhang, J., Zhang, G. S., Bi, Y. F., and Liu, S. M.: Nitrogen species in rainwater and aerosols of the Yellow and East China seas: Effects of the East Asian monsoon and anthropogenic emissions and relevance for the NW Pacific Ocean, Global Biogeochem. Cy., 25, 113-120, 2011.

Zhang, K., and Gao, H. W.: The characteristics of Asian-dust storms during 2000–2002: From the source to the sea, Atmos. Environ., 41, 9136-9145, 2007.

Zhang, Q., Streets, D. G., Carmichael, G. R., He, K. B., Huo, H., Kannari, A., Klimont,Z., Park, I. S., Reddy, S., Fu, J. S., Chen, D., Duan, L., Lei, Y., Wang, L. T., and Yao, Z. L.: Asian emissions in 2006 for the NASA INTEX-B mission. Atmos. Chem. Phys., 9, 5131-5153, 2009.

Zhang, W. J., Zhuang, G. S., Huang, K., Li, J., Zhang, R., Wang, Q. Z., Sun, Y. L., Fu, J. S., Chen, Y., and Xu, D. Q.: Mixing and transformation of Asian dust with pollution in the two dust storms over the northern China in 2006, Atmos. Environ., 44, 3394-3403, 2010a.

Zhang, Y. and Carmichael, G. R.: The role of mineral aerosol in tropospheric chemistry in East Asia - a model study, J. Appl. Meteorol., 38, 353-366, 1999.

Zhang, Y., Sunwoo, Y., Kotamarthi, V. R., and Carmichael, G. R.: Photochemical oxidant processes in the presence of dust: an evaluation of the impact of dust on particulate nitrate and ozone formation, J. Appl. Meteorol., 33, 813-824, 1994.

Zhang, Y., Yu, Q., Ma, W. C., and Chen, L. M.: Atmospheric deposition of inorganic nitrogen to the eastern China seas and its implications to marine biogeochemistry, J. Geophys. Res-Atmos., 115, 3421-3423, 2010b.

689 **Table 1**. Sampling information for the aerosol samples collected at the Baguanshan site in the coastal
690 region of the Yellow Sea.

| Sampling year | Sample category | Sampling number | Sampling time | Weather characteristics |
|---|---|---|---|---|
| 2008 | Samples on dust days | 20080301 | From 13:22 a.m. to 17:22 p.m. on Mar. 1st | Floating dust[a] |
| | | 20080315 | From 13:21 a.m. to 17:21 p.m. on Mar. 15th | Floating dust |
| | | 20080425 | From 13:14 a.m. to 17:14 p.m. on Apr. 25th | Floating dust |
| | | 20080528 | From 11:38 a.m. to 15:38 p.m. on May 28th | Floating dust |
| | | 20080529 | From 10:15 a.m. to 12:15 p. m. on May 29th[b] | Floating dust |
| | Reference Samples | 20080316 | From 13:00 a.m. to 17:00 p.m. on Mar. 16th | Sunny day |
| | | 20080424 | From 13:00 a.m. to 17:00 p.m. on Apr. 24th | Sunny day |
| | | 20080522 | From 13:00 a.m. to 17:00 p.m. on May 22nd | Cloudy day with mist |
| 2009 | Samples on dust days | 20090316 | From 8:25 a.m. to 12:25 p.m. on Mar. 16th | Floating dust |
| | Reference Samples | 20090306 | From 13:00 a.m.to 17:00 p.m. on Mar. 6th | Sunny day |
| 2010 | Samples on dust days | 20100315 | From 11:30 a.m.to 15:30 p.m. on Mar. 16th | Mist after floating dust |
| | | 20100320 | From 10:30 a.m. to 14:30 p.m. on Mar. 20th | Floating dust |
| | | 20100321 | From 10:30 a.m. to 14:30 p.m. on Mar. 21st | Floating dust |
| | Reference Samples | 20100324 | From 11:30 a.m. to 15:30 p.m. on Mar. 24th | Sunny day |
| 2011 | Samples on dust days | 20110319 | From 12:00 a.m. to 16:00 p.m. on Mar. 19th | Floating dust |
| | | 20110415 | From 12:00 a.m. to 16:00 p.m. on Apr. 15th | Floating dust |
| | | 20110418 | From 12:25 a.m. to 16:25 p.m. on Apr. 18th | Floating dust[c] |
| | | 20110501 | From 12:10 a.m. to 16:10 p.m. on May 1st | Floating dust |
| | | 20110502 | From 16:00 a.m. to 20:00 p.m. on May 2nd | Floating dust |
| | Reference Samples | 20110308 | From 12:00 a.m. to 16:00 p.m. on Mar. 8th | Sunny day |

| | | | |
|---|---|---|---|
| | 20110416 | From 12:00 a.m. to 16:00 p.m. on Apr. 16th | Sunny day |
| | 20110523 | From 12:00 a.m. to 16:00 p.m. on May 23rd | Sunny day |

[a]Note that one dust sample 20080301 was collected on March 1 when no dust was recorded by the MICAPS. However, the MICAPS information indeed showed dust events in China on March 1. The modeled spatial distribution of the $PM_{10}$ mass concentration for this dust event on March 1 implies that the sample should be classified as a dust sample. The supporting figures are shown in Fig. S1.

[b]The sampling duration was reduced to only 2 hrs because of extremely high particle loads. In addition, the samples with IDs of 20080528 and 20080529 were subjected to two different dust events occurring over two days instead of continuous samples for one dust event (CMA, 2009).

[c]Note that one dust sample 20110418 was collected on April 18 when no dust was recorded by the MICAPS. However, blowing dust occurred and was recorded on April 17 by the Sand-dust Weather Almanac 2011 (CMA, 2013). The modeled spatial distribution of the $PM_{10}$ mass concentration for this dust event on April 18 implies that the sample should be classified as a dust sample. The supporting figure is Fig. S2.

731 **Table 2.** Detection limits, precisions and recoveries of water-soluble ions and metal elements.

| Component | Measurement method | Detection limit ($\mu g\ L^{-1}$) | Precision (RSD%) | Recovery (%) |
|---|---|---|---|---|
| $NO_3^-$ | IC | 2.72 | 1.54 | 97 |
| $SO_4^{2-}$ | | 1.62 | 1.55 | 98 |
| $NH_4^+$ | | 0.4 | 1.10 | 97 |
| $Ca^{2+}$ | | 0.44 | 0.79 | 94 |
| Cu | ICP-MS (Xin et al., 2012) | 0.006 | 4.0 | 106 |
| Zn | | 0.009 | 2.5 | 102 |
| Cr | | 0.004 | 3.0 | 95 |
| Sc | | 0.002 | 2.4 | 97 |
| Pb | | 0.008 | 3.9 | 104 |
| Al | ICP-AES (Lin et al., 1998) | 7.9 | 0.6 | 103 |
| Ca | | 5.0 | 1.2 | 99 |
| Fe | | 2.6 | 0.7 | 104 |
| Na | | 3.0 | 0.6 | 99 |
| Mg | | 0.6 | 0.6 | 105 |
| Hg | CVAFS | 0.0001 | 6.6 | 105 |
| As | CVAFS | 0.1 | 5.0 | 98 |

732
733
734
735
736
737
738
739
740
741
742
743
744
745
746
747
748
749
750
751
752
753
754
755
756

**Table 3.** The average concentrations and EFs of metal elements on dust and non-dust days.

| Element | Concentration ($ng/m^3$) | | EF* | |
|---|---|---|---|---|
| | Reference days | Dust days | Reference days | Dust days |
| Sc | 1.11 | 13.90 | - | - |
| Al | $8.53\times10^3$ | $6.86\times10^4$ | 3.8 | 1.4 |
| Fe | $4.91\times10^3$ | $3.88\times10^4$ | 3. | 1.2 |
| Ca | $1.05\times10^4$ | $4.29\times10^4$ | 14.0 | 2.1 |
| Mg | $1.62\times10^3$ | $1.58\times10^4$ | 3.5 | 1.1 |
| Cu | 50.2 | 124.5 | 36.3 | 6.1 |
| Pb | 127.9 | 221.0 | 389.4 | 56.1 |
| Zn | 340.0 | 457.7 | 248.9 | 20.6 |
| Cr | 33.8 | 244.0 | 44.0 | 11.1 |
| Hg | 0.26 | 0.36 | 176.0 | 13.8 |
| As | 25.5 | 27.4 | 707.2 | 43.9 |

*EF values less than 10 indicate that the studied element is mainly derived from crustal sources, whereas EF values much higher than 10 indicate an anthropogenic source.

788 **Table 4.** Average measured concentrations of $NH_4^+$, $NO_3^-$, TSP, NOx, relative humidity (RH) and air
789 temperature for each aerosol sample category in Qingdao.

| | Sample number | TSP ($\mu g \cdot m^{-3}$) | $NO_3^-$ ($\mu g \cdot m^{-3}$) | $NH_4^+$ ($\mu g \cdot m^{-3}$) | RH (%) | T (℃) | NOx ($\mu g \cdot m^{-3}$) | Summary |
|---|---|---|---|---|---|---|---|---|
| Category 1 | 20080301 | 527 | 20.5 | 12.7 | 57 | 7.0 | 36 | $NH_4^+$ and $NO_3^-$ concentration in dust day samples higher than reference samples |
| | 20080315 | 410 | 19. 5 | 29.9 | 62 | 11.0 | 59 | |
| | 20090316 | 688 | 15.9 | 17.2 | 27 | 16.0 | 75 | |
| | 20100321 | 519 | 16.5 | 9.4 | 51 | 8.8 | 76 | |
| | 20110502 | 810 | 21.0 | 11.0 | 49 | 17.7 | 62 | |
| Category 2 | 20080425 | 622 | 6.8 | 2.0 | 30 | 18.0 | 40 | $NH_4^+$ and $NO_3^-$ concentration in dust day samples lower than reference samples |
| | 20080528 | 2579 | 9.2 | 2.7 | 17 | 27.0 | 34 | |
| | 20080529 | 2314 | 17.5 | 4.8 | 60 | 20.0 | 29 | |
| | 20110319 | 939 | 12.3 | 9.4 | 16 | 12.6 | 93 | |
| | 20110501 | 502 | 4.5 | 5.3 | 23 | 21.6 | 66 | |
| Category 3 | 20100315 | 501 | 5.4 | 4.3 | 30 | 7.2 | 73 | $NO_3^-$ concentration in dust day samples lower than reference samples; $NH_4^+$ close to that on reference samples |
| | 20100320 | 3857 | 5.5 | 3.4 | 35 | 10.6 | 92 | |
| | 20110418 | 558 | 3.8 | 6.6 | 33 | 12.6 | 47 | |
| Reference samples[a] | 20080316 | 225 | 12.6 | 8.4 | 28 | 11.0 | 60 | |
| | 20080424 | 137 | 21.7 | 7.2 | 49 | 18.0 | 53 | |
| | 20080522 | 206 | 27.4 | 16.6 | 78 | 20.0 | 60 | |
| | 20090306 | 94 | 2.9 | 3.0 | 29 | 7.00 | 51 | |
| | 20100324 | 275 | 7.2 | 2.4 | 23 | 9.0 | 82 | |
| | 20110308 | 194 | 13.0 | 13.1 | 20 | 11.5 | 111 | |
| | 20110416 | 252 | 5.6 | 5.4 | 26 | 14.1 | 55 | |
| | 20110523 | 224 | 15.2 | 10.2 | 42 | 20.6 | 49 | |

790 [a]For the corresponding reference sample for each dust event, see Table 1.
791
792

**Table 5.** Comparison of the $NH_4^+$ and $NO_3^-$ content in sand and aerosol particles on dust days or close to the dust source region (unit: μg/g).

| Sands sampled in dust source regions | | | Aerosols in or close to dust source region on dust days | | | Aerosols in the coastal region of the Yellow Sea | |
|---|---|---|---|---|---|---|---|
| Study region and data source | Relative concentration[a] | | Study region and data source | Relative concentration[a] | | | |
| | $NO_3^-$ | $NH_4^+$ | | $NO_3^-$ | $NH_4^+$ | $NO_3^-$ | $NH_4^+$ |
| Zhurihe (This study) | 25.46 ± 22.87 | 4.21 ± 1.03 | Duolun (Cui, 2009) | 1200 | 900 | Reference samples: 28,200 ±24,819 | Reference samples: 24,063 ±21,515 |
| Alxa Left Banner, Inner Mongolia (Niu and Zhang, 2000) | 62.1 ±7.4 | 79.1 ±1.1 | Alxa Right Banner, Inner Mongolia (Niu and Zhang, 2000) | 1975[b] | 4091[b] | Category 1: 34,892 ±9570 | Category 1: 22,571 ±7,016 |
| Yanchi, Ningxia (Niu and Zhang, 2000) | 46.4 ±2.2 | 80.9 ±1.3 | Hinterland of the Taklimakan Desert, Xinjiang (Dai et al., 2016) | 142-233 | 2-15 | Category 2: 5,542 ±5,117 | Category 2: 4,758 ±5,698 |
| | | | Average of Sonid Youqi, Huade (Inner Mongolia), Zhangbei (Hebei) (Mori et al., 2003) | 253 | 710 | Category 3: 6,359 ±4,697 | Category 3: 7,059 ±5,591 |
| | | | Yulin, the north edge of Loess Plateau (Wang et al., 2011) | 216.4 | 80.6 | | |
| | | | Golmud, Qinghai(Sheng et al., 2016) | 892.9 | -[c] | | |
| | | | Hohhot, Inner Mongolia (Yang et al., 1995) | 588.1 | No data | | |

[a]Relative concentration of $NH_4^+$ and $NO_3^-$ per aerosol particle mass

[b]Samples collected on a floating dust day (horizontal visibility less than 10000 m and very low wind speed)

[c]The ammonium concentration was lower than the detection limit of the analytical instrument.

**Table 6.** Sources and source contributions (expressed in %) calculated for aerosol samples collected during dust and non-dust events

| Dust event | | Comparison days | |
|---|---|---|---|
| Source | % of TSP | Source | % of TSP |
| Soil dust | 36 | Soil dust | 23 |
| Industrial | 21 | Industrial | 24 |
| Secondary aerosol | 6 | Secondary aerosol | 23 |
| Oil combustion | 6 | Biomass burning | 16 |
| Coal combustion and other uncertain sources | 31 | Coal combustion | 5 |
| | | Sea salt | 9 |

**Table 7.** Concentrations of TSP, $NO_3^-$, and $NH_4^+$; transport speed; transport distance over the sea; transport distance; air temperature; RH; average mixed layer during transport and transport time in polluted region for atmospheric aerosol samples on dust days.

| Group | Sample number | TSP ($\mu g/m^3$) | $NO_3^-$ ($\mu g/g$) | $NH_4^+$ ($\mu g/g$) | Speed (km/h) | Distance over the sea (km) | Transport altitude (m) | Mixed layer depth (m) | R-time[a] (h) | T[b] (℃) | RH[c] (%) |
|---|---|---|---|---|---|---|---|---|---|---|---|
| Category 1 $NH_4^+$ >RS[d] $NO_3^-$ >RS[d] | 080301 | 527 | 38,984 | 24,107 | 40.1 | 0 | 1,160±702 | 864±745 | 39 | -2.9±11.7 | 29±10 |
| | 080315 | 410 | 47,611 | 34,130 | 79.1 | 0 | 4,921±1,870 | 950±525 | 13 | -32.5± 16.4 | 34±16 |
| | 090316 | 688 | 23,050 | 25,012 | 86.2 | 0 | 3,739±1083 | 702±665 | 11 | -19.1±11.7 | 42±17 |
| | 100321 | 519 | 31,741 | 18,155 | 87.2 | 0 | 3,407±1,249 | 1,113±760 | 19 | -23.0±13.6 | 42±22 |
| | 110502 | 810 | 25,995 | 13,632 | 30.2 | 177 | 3,666±1,371 | 747±957 | 26 | -13.2±15.8 | 31±13 |
| Category 2 $NH_4^+$ <RS[d] $NO_3^-$ <RS[d] | 080425 | 256 | 4,089 | 372 | 29.6 | 0 | 887±656 | 1,161±1,040 | 10 | -2.7±6.1 | 66±13 |
| | 080528 | 2579 | 232 | 72 | 88.2 | 244 | 4,336±1461 | 1,064±830 | 8 | -15.5±13.6 | 31±16 |
| | 080529 | 2314 | 26 | 166 | 63.7 | 94 | 2,148±1,725 | 1,194±816 | 43 | 3.6±18.4 | 25±17 |
| | 110319 | 939 | 13,088 | 10,067 | 70.6 | 132 | 4,271±1867 | 790±719 | 27 | -26.3±20.0 | 48±32 |
| | 110501 | 502 | 8,924 | 10,631 | 35.1 | 252 | 3,212±810 | 916±1,114 | 5 | -13.4±8.5 | 39±13 |
| Category 3 $NO_3^-$ <RS[d] $NH_4^+$ ≅RS[d] | 100315 | 501 | 10,767 | 8,515 | 57.3 | 0 | 5,009±1410 | 1,110±365 | 7 | -40.4±13.3 | 45±29 |
| | 100320 | 3857 | 1,418 | 884 | 76.9 | 0 | 1,284±401 | 525±371 | 10 | -12.2±6.3 | 61±16 |
| | 110418 | 558 | 6,891 | 11,778 | 35.6 | 931 | 1,344±780 | 695±672 | 2 | -0.1±8.2 | 52±28 |

[a]Residence time of the air mass passing over parts of highly polluted regions according to the trajectories of samples.

[b]Average air temperature with the definition in Section 2.4.

[c]Average relative humidity with the definition in Section 2.4.

[d]Reference samples collected on days immediately before or after dust event

**Table 8.** Dry deposition of TSP (mg/m$^2$/month), $N_{NH4++NO3-}$ (mg N/m$^2$/month) and some toxic trace metals (mg/m$^2$/month) on dust and reference days.

| | Dry deposition flux | | | | | | | |
|---|---|---|---|---|---|---|---|---|
| | TSP | $NO_3^-$-N | $NH_4^+$-N | $N_{NH4++NO3-}$ | Fe | Cu | Pb | Zn |
| Category 1[a] | 8,000 ± 1800 | 65 ±9 | 24 ±14 | 90 ±17 | 533 ±179 | 2 ±0.3 | 0.3 ±0.3 | 6 ±2 |
| Category 2[a] | 18000 ± 11,000 | 13 ±18 | 8 ±4 | 21 ±22 | 1300 ±1000 | 3 ±2 | 0.08 ±0.04 | 4 ±1 |
| Category 3[a] | 29,000 ± 31,000 | 26 ±6 | 17 ±8 | 42 ±12 | 2100 ±2200 | 6 ±1 | 0.20 ±0.02 | 5 ±3 |
| Reference samples | 2,800 ± 700 | 48 ±33 | 15 ±8 | 63 ±39 | 190 ±110 | 1 ±1 | 0.09 ±0.1 | 5 ±4 |

[a]For the characterization of $N_{NH4++NO3-}$ concentration and sample information of the category, see Table 3.

888 **Table 9.** Comparison of dry deposition flux and normalized flux of TSP (mg/m$^2$/month) and $N_{NH4++NO3}$-
889 (mg N/m$^2$/month) with observations from other studies (mg N/m$^2$/month)

| Source | Year | Area | | TSP | $N_{NH4++NO3}$- | Normalized average flux of $N_{NH4++NO3}$-[a] |
|---|---|---|---|---|---|---|
| This work | 2008-2011 | Qingdao, coastal region of the Yellow Sea | Reference day | 2,800±700 | 63±39 | 93.90 |
| | | | Dust day | 10,138±15,940 | 58±36 | 101.39 |
| | | | Average of dust and reference | | | 97.64 |
| Qi et al., 2013 | 2005-2006 | Qingdao, coastal region of the Yellow Sea | Average of nine months samples | 159.2 - 3,172.9 | 1.8-24.5 | 94.75 |
| Zhang et al., 2011 | 1997-2005 | Qingdao | Average of annual samples | | 132 | 99.65 |
| Zhang et al., 2007 | 1999-2003 | The Yellow Sea | | | 11.43 | 9.91 |
| Shi et al., 2013 | 2007 | The Yellow Sea | Reference day | | 19.2 | 132.17 |
| | | | Dust day | | 104.4 | 227.07 |
| | | | Average of dust and reference | | | 179.62 |

890 [a]The calculation method of the normalized flux of $N_{NH4++NO3}$- was discussed in Section 3.7.
891
892
893
894
895
896
897

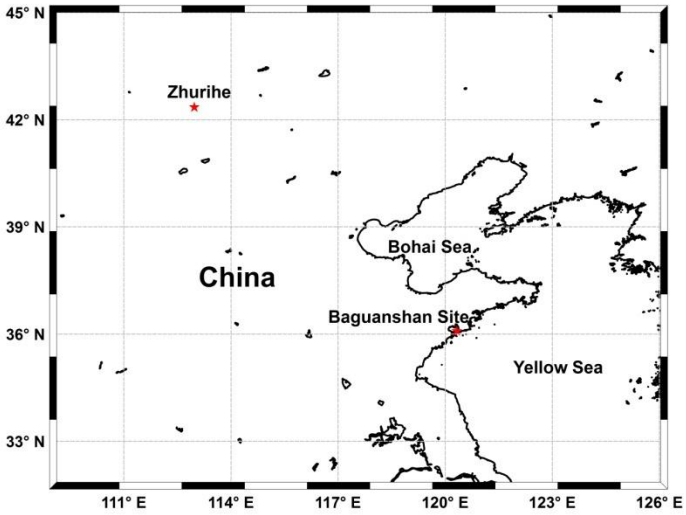


**Figure 1.** Location of the aerosol and dust sampling sites.

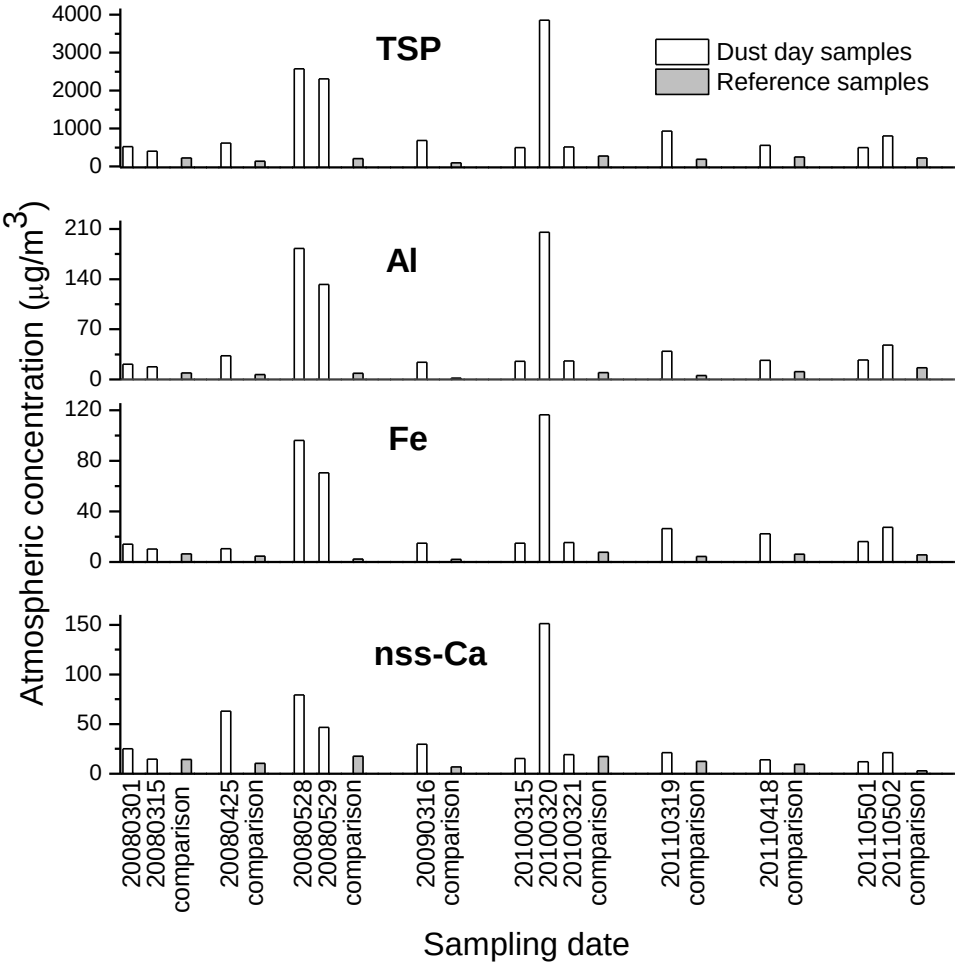


**Figure 2.** Mass concentrations of TSP, Al, Fe and nss-Ca in aerosol samples collected at the Baguanshan site on dust and reference days from 2008 to 2011.

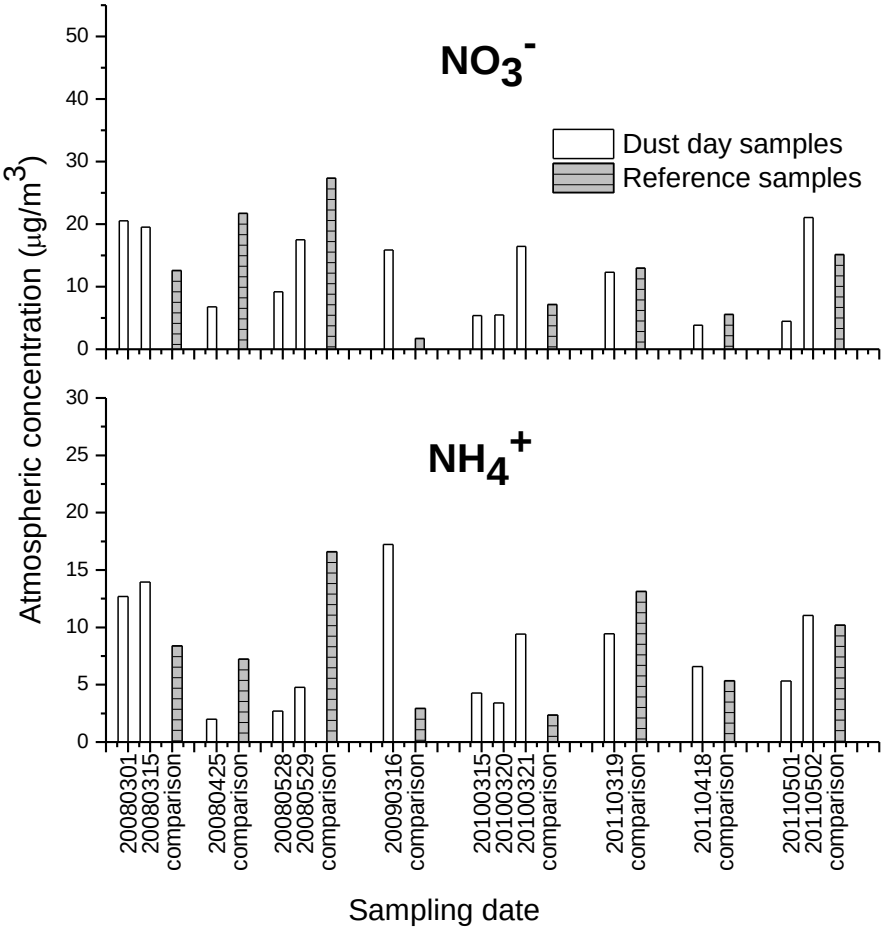


**Figure 3**. Mass concentrations of $NH_4^+$ and $NO_3^-$ in aerosol samples collected at the Baguanshan site on dust and reference days during March-May in 2008 to 2011.

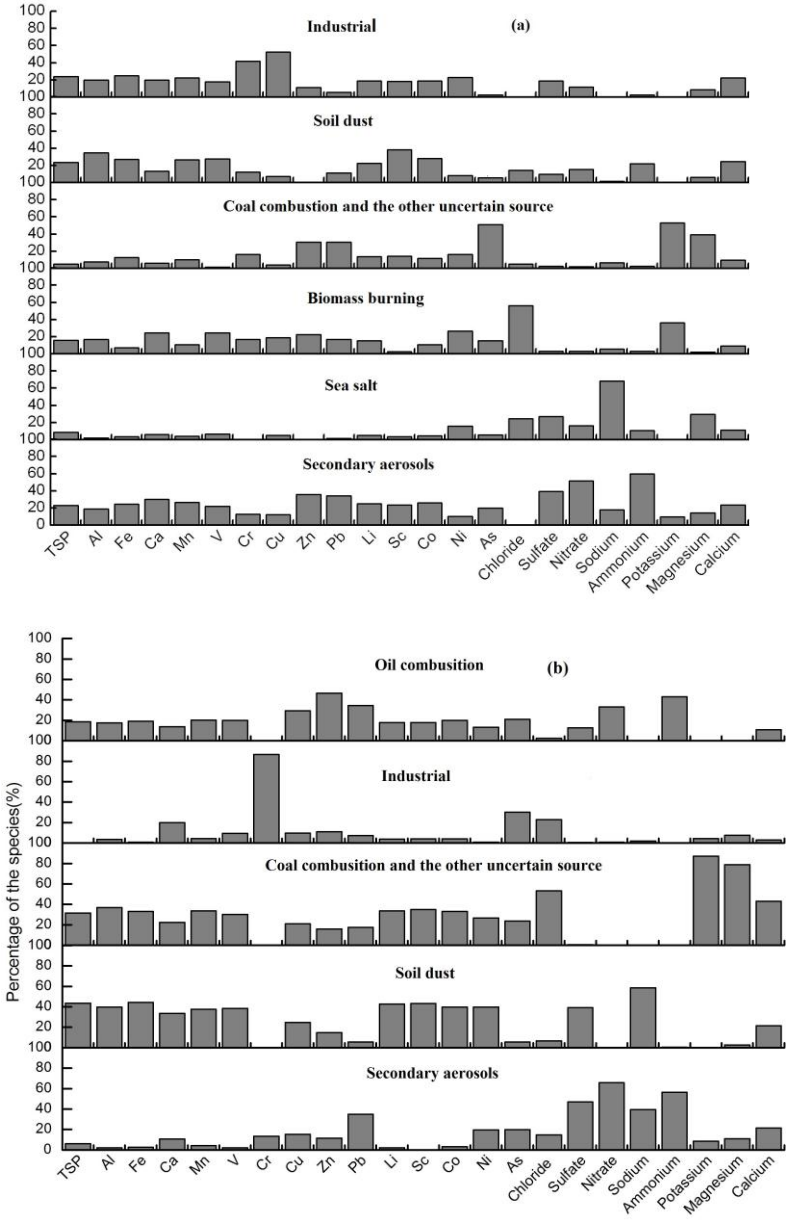


**Figure 4.** Source profiles of atmospheric aerosol samples collected on reference (a) and dust (b) days using the PMF model.

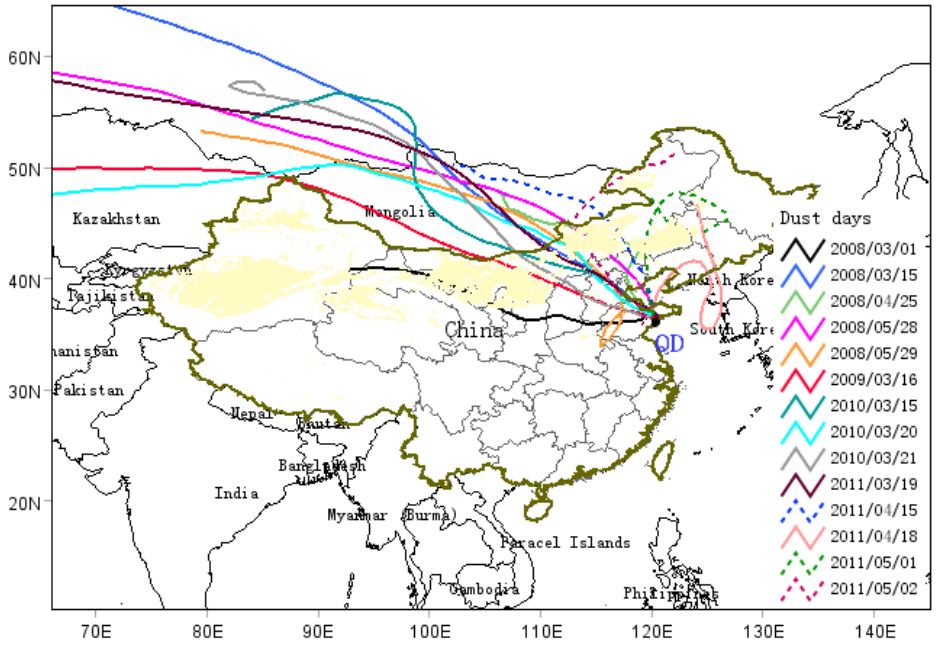


**Figure 5.** The 72-h backward trajectories for dust samples from 2008 to 2011 (the yellow domains in the map represent the dust source regions in China).

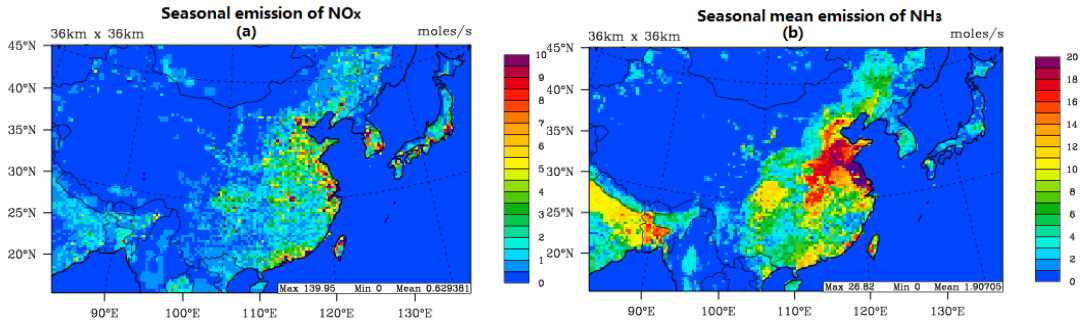


**Figure 6.** Seasonal mean emissions of NOx (a) and $NH_3$ (b) over East Asia from March-May 2008.